Jurnal Tribologi 43 (2024) 57-70

MYTRIBOS Malaysian Tribology Society

Jurnal Tribologi

Website : jurnaltribologi.mytribos.org e-issn: 2289-7232

# Loading and unloading behaviour of an elastic-plastic contact in the presence of trapped fluid interference: biomechanical implications

M. Danny Pratama Lamura [1,3,4], Muhammad Imam Ammarullah [1,4], Mohamad Izzur Maula [1,4], Taufiq Hidayat [2], Hasyid Ahmad Wicaksono [1,4], Michael Ambarita [1], Athanasius Priharyoto Bayuseno [1], J. Jamari [1,4*]

[1] Department of Mechanical Engineering, Universitas Diponegoro, Semarang 50275, Central Java, INDONESIA.
[2] Department of Mechanical Engineering, Universitas Muria Kudus, Kudus 59324, Central Java, INDONESIA.
[3] Department of Mechanical Engineering, Universitas Pembangunan Nasional Veteran Jawa Timur, Surabaya 60294, East Java, INDONESIA.
[4] Undip Biomechanics Engineering & Research Centre (UBM-ERC), Universitas Diponegoro, Semarang 50275, Central Java, INDONESIA.
[*]Corresponding author: j.jamari@gmail.com

KEYWORDS

Contact mechanics
Elastic-plastic
Sinusoidal
Trapped fluid
Loading-unloading

ABSTRACT

This study examines the biomechanical implications of lubricants trapped in deformable sinusoidal valleys under loading and unloading against rigid flats using the finite element method (FEM). This phenomenon is similar to the intervertebral discs in the spine under loading-unloading conditions. Materials are assumed to be elastic-perfectly plastic, and lubricants are modelled as either compressible or incompressible. The contact area, deformation, and von Mises stress have been discussed in this study. The result showed good agreement with the past research in the dry conditions and the trapped fluid in the incomplete filling during loading conditions. The incomplete filling is the condition of the sinusoidal valley volume being bigger than the lubricant volume. Additional lubricant reduces the contact area and deformations in the loading conditions while shrinking the von Mises stress distribution. For dry and lubricated contact, the most significant decline in contact area, deformation, and von Mises stress distribution is observed in incompressible conditions. Additional lubricant reduces contact area and deformations and shrinkage of the von Mises stress distribution in the complete filling. The findings are necessary for understanding joint mechanics and the durability of biomedical implants.

Received 16 July 2024; received in revised form 18 October 2024; accepted 3 November 2024.
To cite this article: Lamura et al., (2024). and unloading behaviour of an elastic-plastic contact in the presence of trapped fluid interference. Jurnal Tribologi 43, pp.57-70.

## 1.0 INTRODUCTION

Contact mechanics are challenging conditions to avoid failure (Öner et al., 2022; Yaylacı et al., 2022). The moment two solids came into contact, the load was applied in normal and tangential conditions, which caused the failure (Boucly et al., 2007; X. Wang et al., 2017; Yaylaci, Abanoz, et al., 2022; Yaylacı et al., 2022). Most of the contact mechanics analysis is loading. In real-world conditions, loading-unloading with multiple cycles always happens especially in biomechanics problems. Consequently, studying loading-unloading contact is essential to predict the lifetime and when to maintain engineering products. To determine the service life of a structure, it is necessary to decide on the damage that will occur at its contact points and avoid cracks in the structure (Özdemir & Yaylaci, 2023; Yaylaci et al., 2023; Yaylaci, Yaylaci, et al., 2022). The contact problem can be solved using experimental, analytic, and numerical approaches (H. Wang et al., 2017; Yaylaci, 2016, 2022).

The study of loading-unloading contact is mainly in the asperity contact model. The conformal geometry has been used in the asperity contact models such as spherical, elliptical, and sinusoidal. The reason for using conformal geometry is to simplify the analysis from the peak of surface roughness. The first study of asperity contact models in the loaded condition by Hertzian models analysis in the elastic material (Fischer-Cripps, 2000). The metal will undergo elastic and plastic contact. The asperity contact has many aspects to analyze, such as material properties and boundary conditions. From the material perspective, JG (R. L. Jackson & Green, 2005), KE (Kogut & Etsion, 2002), YT (You & Tang, 2022), Chen et al. (Chen et al., 2022) are extending the analysis of elastic-plastic material. Furthermore, in the boundary conditions, (R. Jackson et al., 2005), and (Zhao et al., 2015) have extended the analysis to the unloaded condition. The loading-unloading has been extended to multiple cycles, such as Wang et al. (J. Wang et al., 2018), Kadin et al. (Kadin et al., 2006), and CS (Chatterjee & Sahoo, 2013). However, that research neglects friction and lubricant, where friction and lubricant are found in most engineering products.

Engineering surfaces were rough, and the peak of surface roughness is called asperity (Z. J. Wang et al., 2010). The contact of two engineering surfaces occurred because of asperity contact (Chang & Zhang, 2005; Taylor, 2022). The lubricant is a function that separates the surfaces (Bijani et al., 2019; Soltz et al., 2003). However, in the heavy load and the effect of heating as a cause of loading-unloading with multiple cycles, the separation from the lubricant becomes thin, and some of the asperities will come into contact (Zwicker et al., 2022). The between asperities have trapped the lubricant, and the contact phenomenon is interesting to investigate. Because the trapped fluid is found in the human body such as nucleus pulposus of the spine (Mustafy et al., 2014; Wang MD et al., 2018), or to the joints (Ferguson et al., 2000; Kumaresan et al., 1998)and eyes (Huang et al., 2020).

Several researchers have studied the trapped lubricant, such as Kudo et al. reported the lubricant had reduced friction at the tool-work interface, and the hydrostatic pressure from the trapped lubricant supports contact pressure for low friction (Kudo, 1965). Normal pressure and bulk modulus affect the contact area for trapped lubricant conditions (Nellemann et al., 1977). Bulk modulus indicates that the lubricant is a compressible fluid. Nielsen et al. studied the asperity flattening with entrapped lubricant under bulk deformation with new specimen design, friction differences with and without trapped oil (Nielsen et al., 2022). SY has reported the elastic-plastic problem (Shvarts & Yastrebov, 2018). However, the study of trapped fluid in the loading-unloading conditions is limited.

The present study extended the SY analysis of contact interfaces of trapped fluid in loading-unloading conditions. The contact mechanics investigation concerns contact area, deformation,

fluid pressure, and von Mises stress loading process. This study could serve as a preliminary investigation into trapped fluid under multiple-cycling loading. Understanding loading-unloading behaviour is useful in solving biomechanics problems such as cartilage and intervertebral disc which is crucial for predicting their performance and longevity under physiological conditions.

## 2.0 MATERIAL AND METHODS

In this study, the geometry of the contact problem is shown in Figure 1. The sinusoidal geometry was generated using SolidWorks using equations from SY (Shvarts & Yastrebov, 2018), Westergaard (Westergaard, 1939), and Kuznetsov (Kuznetsov, 1985). The sinusoidal models created a plane and imported it to the finite element software with the exported file (.stl). The finite element analysis using Abaqus CAE software to solve the contact problem. The three-dimensional (3D) analysis is comprehensive. Accurate results and versatile application, while disadvantages of 3D are complex setup and high computational time (Corda, Chethan, Bhat N, et al., 2023; Corda, Chethan, Satish Shenoy, et al., 2023; Göktaş et al., 2022; Reginald et al., 2023). This study used the two-dimensional (2D) planar for cost-effective, simple and faster analysis, and the models are ideal for planar problems (Yaylaci et al., 2024). The element CPS4 was used to solve the contact problem.

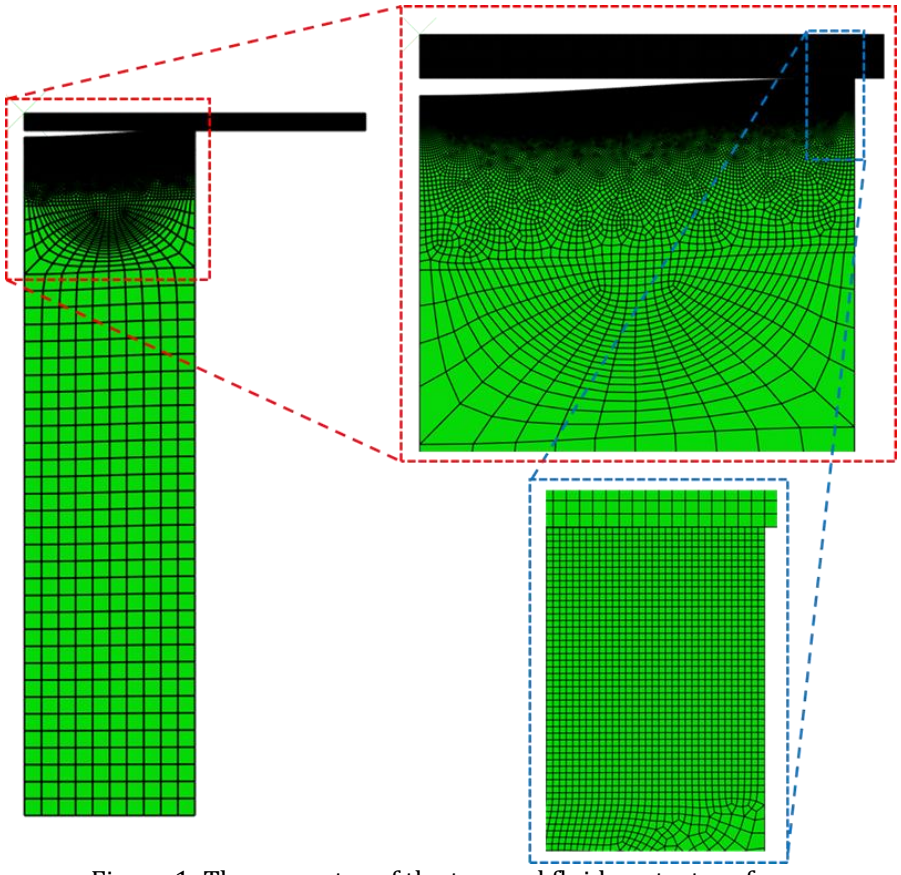

Figure 1: The geometry of the trapped fluid contact surfaces.

The boundary conditions determined based on the SY (Shvarts & Yastrebov, 2018), where the load was applied as a pressure on the bottom surfaces of the sinusoidal. The rigid flat was fixed in all directions, while the sinusoidal only moved in the axis Y direction. The static general with surface-to-surface contact has been used to solve this problem. The loading-unloading process was modelled using three phases that were carried out continuously. First, the initial phase for lubrication input using a fluid cavity with the lubricant's characteristic compressible or incompressible properties. Second, the load has been applied (loading phase), and third, the load was removed (unloading phase). The details of the solid and liquid material properties are shown in Table 1.

Table 1: The material properties.

| **Properties** | **Item** | **Value** | **Unit** |
|---|---|---|---|
| Solid (Aluminum) | Modulus Elasticity | 70000 | MPa |
| | Poisson Ratio | 0.33 | - |
| | Yield Strength | 240 | MPa |
| Liquid | Density | 1000 | $Kg/m^3$ |
| | Bulk Modulus | 2000 | MPa |

## 3.0 RESULTS AND DISCUSSION

The contact of unloading is the next step of loading contact where the load is removed (Jamari et al., 2007; Jamari & Schipper, 2007). The loading process in the elastic contact can be seen as the contact phenomenon. However, the unloading process mostly neglected the contact phenomenon because elastic contact has a highly reversible characteristic. Elastic-plastic contact is a partially reversible contact phenomenon (Lamura et al., 2024). The finite element analysis (FEA) is of great research interest because of its lower cost, faster analysis, and more effortless depiction of stress distribution than the experimental approach. Study meshing is the first analysis before comparing with experimental or past research results. The study of meshing is to find the ideal mesh to FEA with the criterion that different element sizes or numbers of elements have a deviation of less than 1%. This indicates the mesh no longer affects FEA results and has a faster analysis than the smaller element size. The study of meshing in this study is depicted in Figure 2.

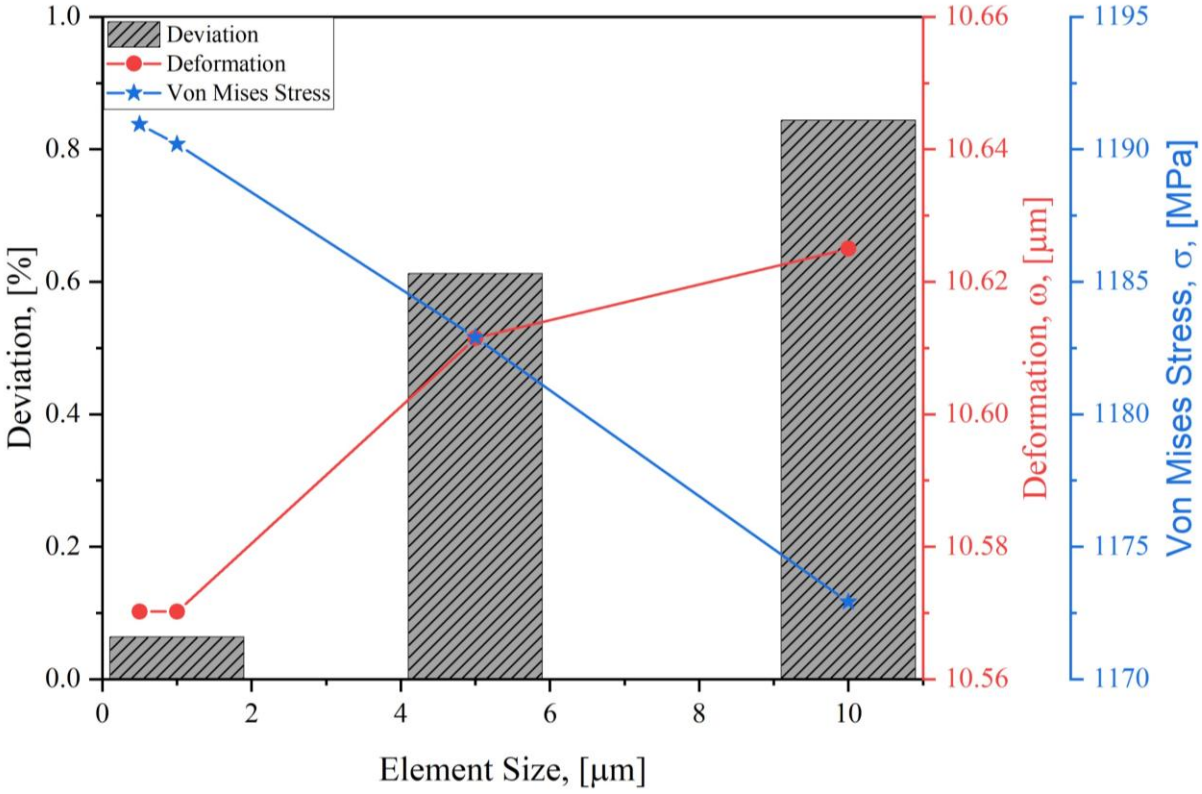


Figure 2: Study of meshing.

The next step of study meshing is validation. The validations of the present study can be compared with experimental or past research results. The present study has been compared with the analytical approach from the FEA results from SY in loading conditions, where this study has extended the previous study in the unloading conditions. Figure 3 shows the contact area against an external load. The present study has been simulated with and without lubricant. The lubricant is modelled as incompressible and compressible. The "Incompressible lubricant-0.9" means the fluid volume is divided by cavity volume. The Present study (NO) agrees well with the SY model. In the incompressible conditions with the ratio volume of lubricant and pocket amount 0.9, have a very good agreement between the SY model and the present study as shown in Figure 3a. The contact area is non-monotonic for external pressure after the fluid has become activated where it is increases and then abruptly decreases, corresponding to the moment fluid pressure has reached the contact pressure and, consequently, permeation has begun (Shvarts & Yastrebov, 2018).

The loading and unloading processes have different contact areas, and the contact area in the loading process is bigger than the unloading process. Because the model still has the elastic part. The elastic makes models reversible and decreases the contact area. However, in this study of an incompressible fluid, when the fluid is activated, the contact area has been the same at $p/E^* = 6.48 \times 10^{-4}$ to $5.26 \times 10^{-3}$ between the loading and unloading process as depicted in the Figure 3b. The different phenomenon has found that the contact area in the unloading process is higher than in

the loading process at $p/E^* \geq 5.26 \times 10^{-3}$. This phenomenon happened because the fluid pressure still has a value before zero. Therefore, the fluid pressure is insignificant to the reduction of the contact area caused by the plasticity material (irreversible) and the increase of the contact area.

Adding lubricant in the trapped conditions reduces the contact area at the ratio volume of fluid and pocket amount 1. The fluid is given to the fluid pressure in all directions, and the pressure has different directions with the external Load as a reason for the contact area decrease. The resultant forces become smaller because the external load has resistance pressure from the fluid pressure. The Resultant forces become smaller, and the contact area (see Figure 3) and deformation (see Figure 4) also decrease. During the loading and unloading phase, a different phenomenon is observed when the volume ratio of fluid to pocket is equal to 1. For the compressible lubricant, the contact area in the loading phase shows a similar trend to that without fluid but with a lower value. In contrast, in the unloading phase, the contact area very close to zero was hard to measure. However, the incompressible at the loading and unloading phase consists of the contact area being zero and the stress concentrated at the peak of the sinusoidal model being considered negligible.

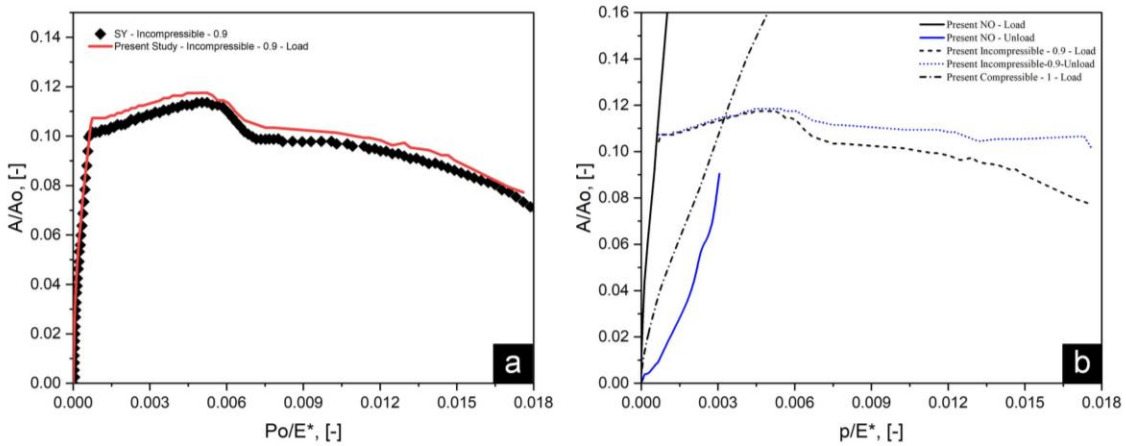


Figure 3: The comparison of the contact area against external Load between: a) the SY model and present study, b) the present study dry and lubricated.

Figure 4 depicts the deformation phenomenon resulting from increasing external load in both lubricated and non-lubricated conditions. As the external load increases, deeper deformations occur in all situations. However, additional lubrication in the cavity distinctly leads to shallower deformation. From an elastic-plastic contact perspective, it is evident that the reduction in resultant forces due to lubrication causes smaller deformations, necessitating a higher external load for plastic deformation to occur. Avoiding plastic deformation is crucial in engineering design as it is often a precursor to failure (Raabe et al., 2025). Therefore, enhancing the accurate detection of plastic deformation can significantly improve efficiency. Adding lubricant remarkably reduces deformation caused by fluid pressure pressing in all directions. Fluid pressure also escalates with increasing external loads, as shown in Figure 5. Acting like a spring, the lubricant undeniably diminishes the applied force (Mang et al., 2010; Nielsen et al., 2022; Zwicker et al., 2022, 2023). From the biomechanical perspective, the incompressible safety lubrication in the intervertebral than compressible, as reported the incompressible lubricant has a small

deformation and reduces the von Mises stress distributions. Mosbah & Bendoukha reported degenerative in the lumbar spine has modelled using compressible fluid (Mosbah & Bendoukha, 2018). The findings of the present study suggest that the higher potential for back pain may be attributed to the behavior of the nucleus pulposus, particularly under conditions where compressible lubricants are present.

The lubrication acting like a spring is resistant to decrease the deformation. The deformation in the unloading process is smaller than the loading process, as the model still exists in the elastic part. In the loading-unloading process, the difference in deformation indicated the spring back of the model had become even in full plastic contact because the maximum stress with the equal value to the yield stress of the material is undistributed to the model overall (Lamura et al., 2024). The distribution of the von Mises stress is shown in Figure 6.

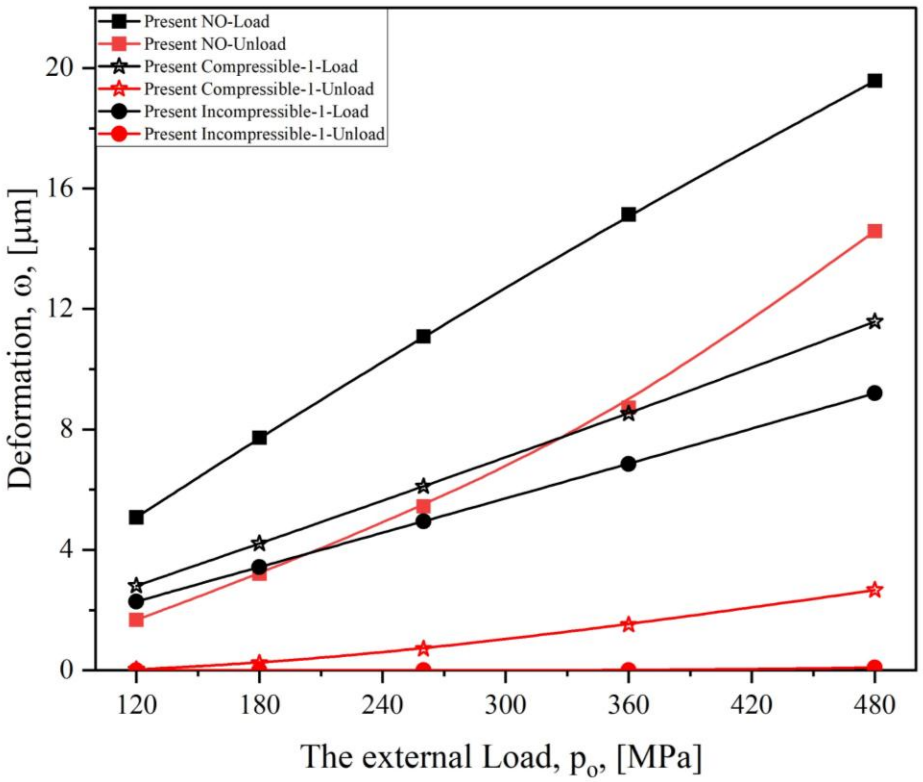


Figure 4: The external Load against deformation in the conditions with and without lubricant.

The investigation into fluid or hydrostatic pressure's impact on external load focuses on the distinction between incompressible and compressible lubricants, as depicted in Figure 5. During the loading process, it is noted that an incompressible lubricant with a volume ratio of 1 displays higher fluid pressure compared to a compressible lubricant. This difference can be attributed to the physical properties of incompressible fluids, which resist changes in volume under pressure. Consequently, when an external load is applied, the pressure within the confined fluid rises significantly. The compressible lubricant, under the same conditions, exhibits lower fluid

pressure. This is due to the capacity of compressible fluids to alter their volume in response to pressure, resulting in less resistance and, therefore, lower pressure buildup.

The fluid pressure in the volume ratio of 1 at the incompressible and compressible lubricants drops to zero, indicating that the trapped fluid is effectively relieved of pressure when the load is removed. This behaviour aligns with the principles of fluid mechanics, where pressure is directly related to the applied load. The increase in trapped fluid pressure during the loading process can be attributed to the physical phenomenon of stress distribution within the material. In all conditions, the fluid pressure rises as the external load is applied, leading to a higher von Mises stress. The von Mises stress measures the yielding criteria for materials under complex loading conditions and plays a critical role in predicting the onset of plastic deformation (R. L. Jackson & Green, 2005). The incompressible lubricant generates higher fluid pressure, resulting in greater von Mises stress. This indicates that the material is more likely to approach its yield point when using an incompressible lubricant under the same loading conditions compared to a compressible one. On the other hand, the compressible lubricant, with its ability to absorb some of the applied load through volume change, results in lower fluid pressure and, subsequently, lower von Mises stress.

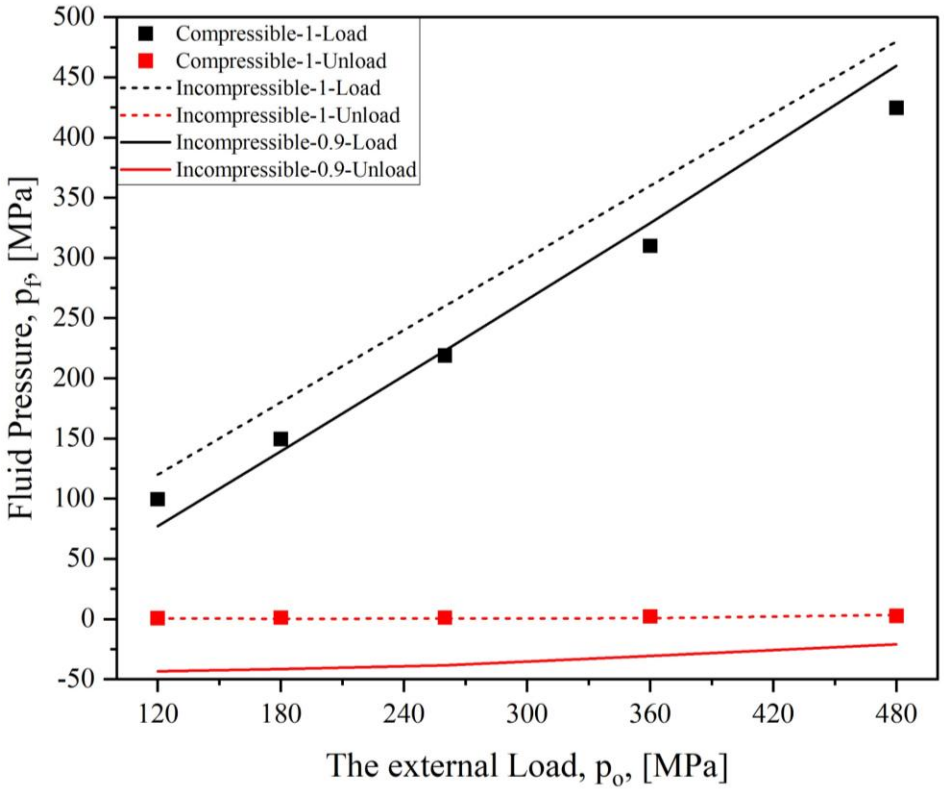


Figure 5: The effect of external Load on fluid pressure.

The goal of the lubricant is to increase the separation of two solid bodies coming into contact (Bijani et al., 2019). However, the full separation of two solid bodies is difficult, especially in the extreme load. The contact area and deformation correspond to an effect of the lubricant

separating the contact problem with a decrease in the contact area and deformation. The von Mises stress distribution becomes smaller when lubricant is added. In the no-fluid condition, the von Mises stress is concentrated in the sinusoidal peak with the solid contact from the rigid flat. Therefore, the compressible lubricant combines the phenomenon of no-fluid and incompressible with a volume ratio equal to 1, where the von Mises stress distribution shrinks compared to the no-fluid. The reduction of concentrated the maximum value of von Mises stress indicates that the solid and liquid contact happens simultaneously.

The incompressible lubricant shows the distribution of von Mises stresses with similar colour, indicating that fluid pressure is distributed in all directions of the cavity surfaces model. As mentioned in the contact area, when the fluid is activated, the contact area increases and decreases at a volume ratio between the fluid and the sinusoidal cavity less than 1. Different results were found when the fluid volume between the fluid and the sinusoidal cavity is equal to 1 in the incompressible fluid where the contact area is zero, as indicated by the fluid being active in the beginning and resisting the contact area. The fluid pressure is distributed over the entire surface, where this phenomenon corresponds to the von Mises stress distribution in Figure 6. The contour shows a similar colour in the distribution of von Mises stress. This provides insight into the trapped lubricant given the fluid pressure under compression, which reduces and spreads the distribution of von Mises stress. This indicates that stress will be spread out the concentrated load in the peak of sinusoidal (see Fig 6. at the NO Fluid) to the entire surface of the cavity, which results in the maximum value stress having a smaller distribution (see Fig. 6 at the incompressible with the volume ratio = 1).

While this study provides valuable insights, the present study has several limitations. First, the material is assumed to be elastic-perfectly plastic which is a simplification compared to more complex material behaviours. Future studies should explore variations in material properties, including strain hardening and anisotropic materials. Second, the model is simplified using 2D planar representation, whereas a 3D model would be necessary to capture more complex interactions accurately. Third, the lubricant is modelled under ideal conditions with constant bulk modulus for compressibility and incompressibility. In real-world conditions, lubricants are compressible with varying bulk modulus, and this variability should be considered in future research. Fourth, the study only considers normal loading and unloading. Future studies should investigate additional loading conditions to provide a more comprehensive understanding such as repeated load (Jamari et al., 2014; Jamari & Schipper, 2008), combined the normal load with tangential load (Kucharski & Starzyński, 2019), and rolling contact (Bogdański & Lewicki, 2008; Miftakhova et al., 2019). These limitations highlight areas for future research to enhance the accuracy and applicability of the findings especially in biomechanics.

## 4.0 CONCLUSIONS

The loading and unloading behaviour of an elastic-plastic contact in the presence of trapped fluid interference has been studied. The study demonstrates that trapped lubricants significantly influence the contact area, deformation, and von Mises stresses under loading conditions. Compared with compressible lubricants, incompressible lubricants display a greater fluid pressure resistance, resulting in a smaller von Mises stress. This indicates a lower likelihood of approaching the material's yield point. The research highlights the differences between the loading and unloading process. Elastic contact is highly reversible, leading to minimal deformation during unloading, while elastic-plastic contact is partially reversible, necessitating

consideration of contact area and deformations. The study confirms that incompressible lubricants with a volume ratio of 0.9 exhibit very good agreement with past research models up to certain pressure levels. However, beyond these levels, deviations occur due to differences in contact area behaviour. Adding lubricant reduces the contact area and deformation, enhancing the separation of contacting surfaces. Lubricants, especially incompressible with a volume ratio of 1, evenly distribute stress, reducing localized stress concentrations and the risk of material failure. The study's limitations, including material simplifications, 2D modelling, idealized lubricant conditions, and the focus on normal loading-unloading, suggest areas for future research. Future studies should explore more complex material behaviours, 3D modelling, real-world lubricant properties, and diverse loading conditions to improve the findings' accuracy and applicability, especially in biomechanics.

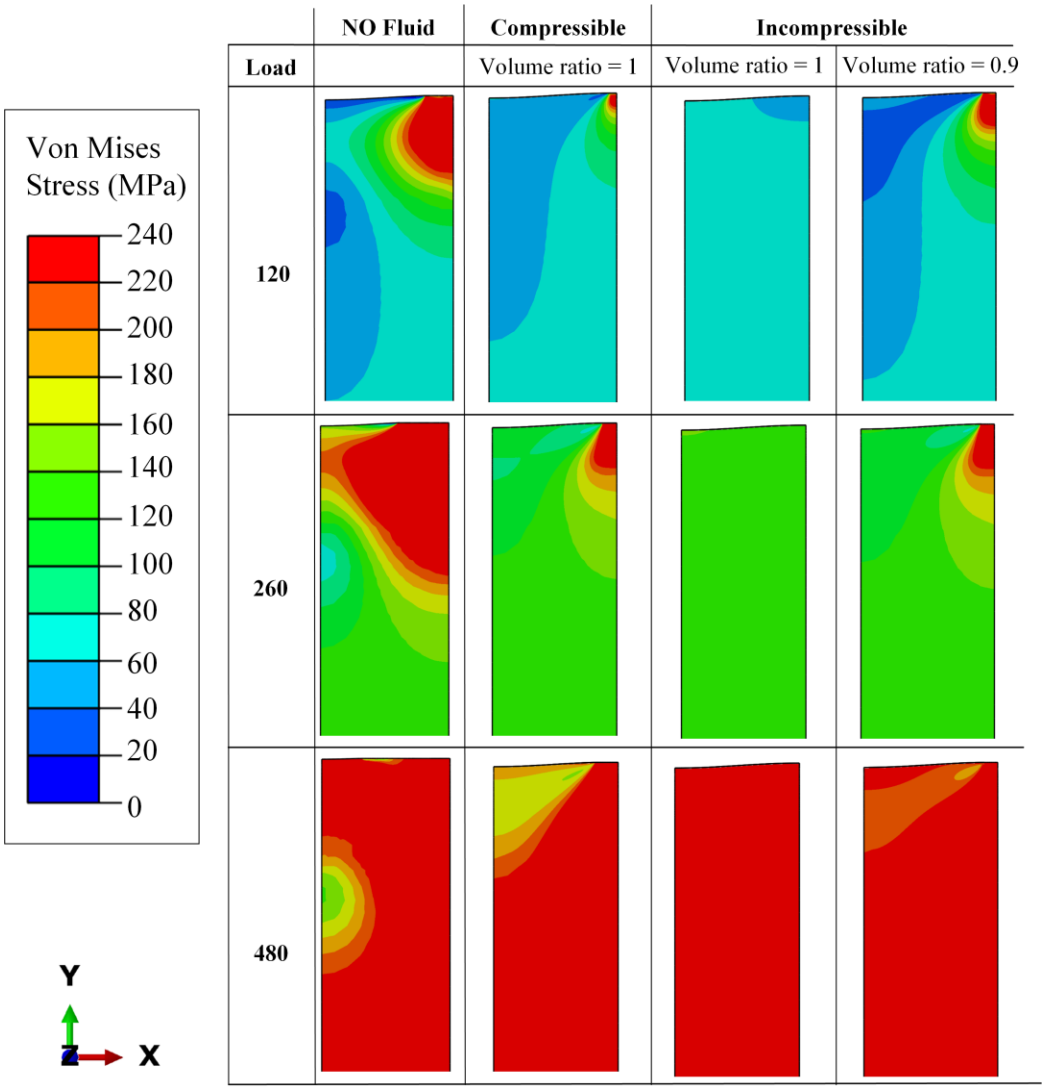


Figure 6: The contour of von Mises stress distribution in the loading process.

**ACKNOWLEDGEMENT**

This work was supported by the Ministry of Education, Culture, Research and Technology of the Republic of Indonesia through a scholarship of the Master Education Program Leading to Doctoral Degree for Excellent Graduates (PMDSU) [grant number: 345-44/UN7.D2/PP/V/2024].

**REFERENCES**

Bijani, D., Deladi, E. L., de Rooij, M. B., & Schipper, D. J. (2019). The influence of surface texturing on the frictional behaviour in starved lubricated parallel sliding contacts. *Lubricants*, *7*(8). https://doi.org/10.3390/lubricants7080068

Bogdański, S., & Lewicki, P. (2008). 3D model of liquid entrapment mechanism for rolling contact fatigue cracks in rails. *Wear*, *265*(9–10), 1356–1362. https://doi.org/10.1016/j.wear.2008.03.014

Boucly, V., Nélias, D., & Green, I. (2007). Modeling of the rolling and sliding contact between two asperities. *Journal of Tribology*, *129*(2), 235–245. https://doi.org/10.1115/1.2464137

Chang, L., & Zhang, H. (2005). On the two points of views of plastically deformed asperity contacts with friction loading. *Proceedings of the Institution of Mechanical Engineers, Part J: Journal of Engineering Tribology*, *219*(3), 201–208. https://doi.org/10.1243/135065005X33883

Chatterjee, B., & Sahoo, P. (2013). Shakedown behavior in multiple normal loading-unloading of an elastic-plastic spherical stick contact. *Tribology in Industry*, *35*(1), 3–18.

Chen, J., Zhang, W., Wang, C., Liu, D., & Zhu, L. (2022). An accurate solution of a hemisphere contact against a rigid flat under varying elastic moduli and yield strengths and comparison with previous model. *Journal of Mechanical Science and Technology*, *36*(9), 4615–4624. https://doi.org/10.1007/s12206-022-0823-1

Corda, J. V., Chethan, K. N., Bhat N, S., Shetty, S., Shenoy B, S., & Zuber, M. (2023). Finite element analysis of elliptical shaped stem profile of hip prosthesis using dynamic loading conditions. *Biomedical Physics and Engineering Express*, *9*(6). https://doi.org/10.1088/2057-1976/acfe14

Corda, J. V., Chethan, K. N., Satish Shenoy, B., Shetty, S., Shyamasunder Bhat, N., & Zuber, M. (2023). Fatigue Life Evaluation of Different Hip Implant Designs Using Finite Element Analysis. *Journal of Applied Engineering Science*, *21*(3), 896–907. https://doi.org/10.5937/jaes0-44094

Ferguson, S. J., Bryant, J. T., Ganz, R., & Ito, K. (2000). The acetabular labrum seal: A poroelastic finite element model. *Clinical Biomechanics*, *15*(6), 463–468. https://doi.org/10.1016/S0268-0033(99)00099-6

Fischer-Cripps, A. C. (2000). Introduction to Contact Mechanics. In *Springer*. Springer-Verlag. https://doi.org/10.1007/b97709

Göktaş, H., Subaşi, E., Uzkut, M., Kara, M., Biçici, H., Shirazi, H., Chethan, K. N., & Mihçin, Ş. (2022). Optimization of Hip Implant Designs Based on Its Mechanical Behaviour. *Lecture Notes in Networks and Systems*, *328 LNNS*(September 2021), 37–43. https://doi.org/10.1007/978-3-030-86297-8_4

Huang, L., Shen, M., Liu, T., Zhang, Y., & Wang, Y. (2020). Inverse solution of corneal material parameters based on non-contact tonometry: A comparative study of different constitutive models. *Journal of Biomechanics*, *112*, 110055. https://doi.org/10.1016/j.jbiomech.2020.110055

Jackson, R., Chusoipin, I., & Green, I. (2005). A Finite Element Study of the Residual Stress and Deformation in Hemispherical Contacts. *Journal of Tribology*, *127*(3), 484–493.

https://doi.org/10.1115/1.1843166
Jackson, R. L., & Green, I. (2005). A finite element study of elasto-plastic hemispherical contact against a rigid flat. *Journal of Tribology*, *127*(2), 343–354. https://doi.org/10.1115/1.1866166
Jamari, J., de Rooij, M. B., & Schipper, D. J. (2007). Plastic deterministic contact of rough surfaces. *Journal of Tribology*, *129*(4), 957–962. https://doi.org/10.1115/1.2768618
Jamari, J., Ismail, R., Saputra, E., Sugiyanto, S., & Anwar, I. B. (2014). The effect of repeated impingement on UHMWPE material in artificial hip joint during salat activities. *Advanced Materials Research*, *896*, 272–275. https://doi.org/10.4028/www.scientific.net/AMR.896.272
Jamari, J., & Schipper, D. J. (2007). Plastic deformation and contact area of an elastic-plastic contact of ellipsoid bodies after unloading. *Tribology International*, *40*(8), 1311–1318. https://doi.org/10.1016/j.triboint.2007.02.015
Jamari, J., & Schipper, D. J. (2008). Deterministic repeated contact of rough surfaces. *Wear*, *264*(3–4), 349–358. https://doi.org/10.1016/j.wear.2007.03.024
Kadin, Y., Kligerman, Y., & Etsion, I. (2006). Multiple loading-unloading of an elastic-plastic spherical contact. *International Journal of Solids and Structures*, *43*(22–23), 7119–7127. https://doi.org/10.1016/j.ijsolstr.2006.03.006
Kogut, L., & Etsion, I. (2002). Elastic-plastic contact analysis of a sphere and a rigid flat. *Journal of Applied Mechanics, Transactions ASME*, *69*(5), 657–662. https://doi.org/10.1115/1.1490373
Kucharski, S., & Starzyński, G. (2019). Contact of rough surfaces under normal and tangential loading. *Wear*, *440–441*(August). https://doi.org/10.1016/j.wear.2019.203075
Kudo, H. (1965). A note on the role of microscopically trapped lubricant at the tool-work interface. *International Journal of Mechanical Sciences*, *7*(5), 383–388. https://doi.org/10.1016/0020-7403(65)90066-4
Kumaresan, S., Yoganandan, N., & Pintar, F. A. (1998). *Finite element modeling approaches of human cervical spine facet joint capsule*. *31*, 371–376.
Kuznetsov, Y. A. (1985). Effect of fluid lubricant on the contact characteristics of rough elastic bodies in compression. *Wear*, *102*(3), 177–194. https://doi.org/10.1016/0043-1648(85)90217-0
Lamura, M. D. P., Ammarullah, M. I., Maula, M. I., Hidayat, T., Bayuseno, A. P., & Jamari, J. (2024). The Effect of Load, Diameter Ratio, and Friction Coefficient on Residual Stress in a Hemispherical Contact for Application in Biomedical Industry. *Journal of Materials Engineering and Performance*. https://doi.org/10.1007/s11665-024-09330-9
Mang, T., Bobzin, K., & Bartels, T. (2010). *Industrial Tribology*. Wiley. https://doi.org/10.1002/9783527632572
Miftakhova, A., Chen, Y. Y., & Horng, J. H. (2019). Effect of rolling on the friction coefficient in three-body contact. *Advances in Mechanical Engineering*, *11*(8), 1–9. https://doi.org/10.1177/1687814019872303
Mosbah, M., & Bendoukha, M. (2018). Anisotropic response of the Holzapfel's constitutive model for the lumbar spine considering degenerative conditions. *Epitoanyag - Journal of Silicate Based and Composite Materials*, *70*(4), 110–114. https://doi.org/10.14382/epitoanyag-jsbcm.2018.20
Mustafy, T., El-rich, M., Mesfar, W., & Moglo, K. (2014). Investigation of impact loading rate effects on the ligamentous cervical spinal load-partitioning using fi nite element model of functional spinal. *Journal of Biomechanics*, *47*(12), 2891–2903. https://doi.org/10.1016/j.jbiomech.2014.07.016
Nellemann, T., Bay, N., & Wanheim, T. (1977). Real area of contact and friction stress - The role of

trapped lubricant. *Wear*, *43*(1), 45–53. https://doi.org/10.1016/0043-1648(77)90042-4

Nielsen, C. V., Zwicker, M. F. R., Spangenberg, J., Bay, N., & Martins, P. A. F. (2022). The role of entrapped lubricant in asperity flattening under bulk plastic deformation. *CIRP Annals*, *71*(1), 241–244. https://doi.org/10.1016/j.cirp.2022.03.001

Öner, E., Şengül Şabano, B., Uzun Yaylacı, E., Adıyaman, G., Yaylacı, M., & Birinci, A. (2022). On the plane receding contact between two functionally graded layers using computational, finite element and artificial neural network methods. *ZAMM - Journal of Applied Mathematics and Mechanics / Zeitschrift Für Angewandte Mathematik Und Mechanik*, *102*(2). https://doi.org/10.1002/zamm.202100287

Özdemir, M. E., & Yaylaci, M. (2023). Research of the impact of material and flow properties on fluid-structure interaction in cage systems. *Wind and Structures*, *36*(1), 31–40. https://doi.org/https://doi.org/10.12989/was.2023.36.1.031

Raabe, D., Tasan, C. C., & Olivetti, E. A. (2025). Strategies for improving the sustainability of structural metals. *Nature*, *575*(November 2019). https://doi.org/10.1038/s41586-019-1702-5

Reginald, J., Kalayarasan, M., Chethan, K. N., & Dhanabal, P. (2023). Static, dynamic, and fatigue life investigation of a hip prosthesis for walking gait using finite element analysis. *International Journal of Modelling and Simulation*, *43*(5), 797–811. https://doi.org/10.1080/02286203.2023.2212346

Shvarts, A. G., & Yastrebov, V. A. (2018). Trapped fluid in contact interface. *Journal of the Mechanics and Physics of Solids*, *119*, 140–162. https://doi.org/10.1016/j.jmps.2018.06.016

Soltz, M. A., Basalo, I. M., & Ateshian, G. A. (2003). Hydrostatic Pressurization and Depletion of Trapped Lubricant Pool During Creep Contact of a Rippled Indenter Against a Biphasic Articular Cartilage Layer. *Journal of Biomechanical Engineering*, *125*(5), 585–593. https://doi.org/10.1115/1.1610020

Taylor, R. I. (2022). Rough Surface Contact Modelling—A Review. *Lubricants*, *10*(5), 1–23. https://doi.org/10.3390/lubricants10050098

Wang, H., Yin, X., Qi, X., Deng, Q., Yu, B., & Hao, Q. (2017). Experimental and theoretical analysis of the elastic-plastic normal repeated impacts of a sphere on a beam. *International Journal of Solids and Structures*, *109*, 131–142. https://doi.org/10.1016/j.ijsolstr.2017.01.014

Wang, J., Li, Q., Yang, C., & Zhou, C. (2018). Repeated loading model for elastic–plastic contact of geomaterial. *Advances in Mechanical Engineering*, *10*(7), 1–15. https://doi.org/10.1177/1687814018788778

Wang MD, K., Jiang PhD, C., Wang PhD, L., Wang MD, H., & Niu PhD, W. (2018). The biomechanical influence of anterior vertebral body osteophytes on the lumbar spine: A finite element study. *Spine Journal*, *18*(12), 2288–2296. https://doi.org/10.1016/j.spinee.2018.07.001

Wang, X., Xu, Y., & Jackson, R. L. (2017). Elastic–Plastic Sinusoidal Waviness Contact Under Combined Normal and Tangential Loading. *Tribology Letters*, *65*(2). https://doi.org/10.1007/s11249-017-0827-7

Wang, Z. J., Wang, W. Z., Hu, Y. Z., & Wang, H. (2010). A numerical elastic-plastic contact model for rough surfaces. *Tribology Transactions*, *53*(2), 224–238. https://doi.org/10.1080/10402000903177908

Westergaard, H. M. (1939). Bearing Pressures and Cracks: Bearing Pressures Through a Slightly Waved Surface or Through a Nearly Flat Part of a Cylinder, and Related Problems of Cracks. *Journal of Applied Mechanics*, *6*(2), A49–A53. https://doi.org/10.1115/1.4008919

Yaylaci, M. (2016). The investigation crack problem through numerical analysis. *Structural*

*Engineering and Mechanics*, *57*(6), 1143–1156. https://doi.org/10.12989/sem.2016.57.6.1143

Yaylaci, M. (2022). Simulate of edge and an internal crack problem and estimation of stress intensity factor through finite element method. *Advances in Nano Research*, *12*(4), 405–414. https://doi.org/https://doi.org/10.12989/anr.2022.12.4.405

Yaylaci, M., Abanoz, M., Yaylaci, E. U., Olmez, H., Sekban, D. M., & Birinci, A. (2022). The contact problem of the functionally graded layer resting on rigid foundation pressed via rigid punch. *Steel and Composite Structures*, *43*(5), 661–672. https://doi.org/https://doi.org/10.12989/scs.2022.43.5.661

Yaylaci, M., Öner, E., Adıyaman, G., Öztürk, Ş., Uzun Yaylacı, E., & Birinci, A. (2024). Analyzing of continuous and discontinuous contact problems of a functionally graded layer: theory of elasticity and finite element method. *Mechanics Based Design of Structures and Machines*, *52*(8), 5720–5738. https://doi.org/10.1080/15397734.2023.2262562

Yaylaci, M., Yaylaci, E. U., Ozdemir, M. E., Ay, S., & Ozturk, Ş. (2022). Implementation of finite element and artificial neural network methods to analyze the contact problem of a functionally graded layer containing crack. *Steel and Composite Structures*, *45*(4), 501–511. https://doi.org/10.12989/scs.2022.45.4.501

Yaylaci, M., Yaylaci, E. U., Ozdemir, M. E., Ozturk, Ş., & Sesli, H. (2023). Vibration and buckling analyses of FGM beam with edge crack: Finite element and multilayer perceptron methods. *Steel and Composite Structures*, *46*(4), 565–575. https://doi.org/https://doi.org/10.12989/scs.2023.46.4.565

Yaylacı, M., Abanoz, M., Yaylacı, E. U., Ölmez, H., Sekban, D. M., & Birinci, A. (2022). Evaluation of the contact problem of functionally graded layer resting on rigid foundation pressed via rigid punch by analytical and numerical (FEM and MLP) methods. *Archive of Applied Mechanics*, *92*(6), 1953–1971. https://doi.org/10.1007/s00419-022-02159-5

You, S., & Tang, J. (2022). A New Model for Sphere Asperity Contact Analysis Considering Strain Hardening of Materials. *Tribology Letters*, *70*(4), 1–12. https://doi.org/10.1007/s11249-022-01668-2

Zhao, B., Zhang, S., Wang, Q. F., Zhang, Q., & Wang, P. (2015). Loading and unloading of a power-law hardening spherical contact under stick contact condition. *International Journal of Mechanical Sciences*, *94–95*, 20–26. https://doi.org/10.1016/j.ijmecsci.2015.02.013

Zwicker, M., Spangenberg, J., Bay, N., Martins, P. A. F., & Nielsen, C. V. (2023). The influence of hydrostatic pressure build-up on asperity flattening under bulk plastic deformation. *Journal of Materials Processing Technology*, *315*(February), 117919. https://doi.org/10.1016/j.jmatprotec.2023.117919

Zwicker, M., Spangenberg, J., Martins, P., & Nielsen, C. V. (2022). Investigation of material strength and oil compressibility on the hydrostatic pressure build-up in metal forming lubricants. *Procedia CIRP*, *115*(March), 78–82. https://doi.org/10.1016/j.procir.2022.10.053